# Electronic Supplementary Information

## Sensitive Sensing of Alkaline Phosphatase and γ-Glutamyltranspeptidase Activity for Tumor Imaging

Yanyun Yang,[a] Miaomiao Zhang,[a] Wenting Zhang,[b] Yinglu Chen,[c] Tong Zhang,[d] Sheng Chen,[a] Yue Yuan,[c] Gaolin Liang,[c] and Shusheng Zhang*,[a]

[a]College of Chemistry, Zhengzhou University, 100 Kexue Road, Zhengzhou, Henan 450001, China.

[b]School of Ecology and Environment, Zhengzhou University, 100 Kexue Road, Zhengzhou, Henan 450001, China.

[c]Department of Chemistry, University of Science and Technology of China, 96 Jinzhai Road, Hefei, Anhui 230026, China

[d]School of Life Sciences, University of Science and Technology of China, 443 Huangshan Road, Hefei, Anhui 230027, China

**Contents:**

## 1. Syntheses and Characterizations of Luc and P-Bz-Luc

***Scheme S1.*** Synthetic route for Luc.

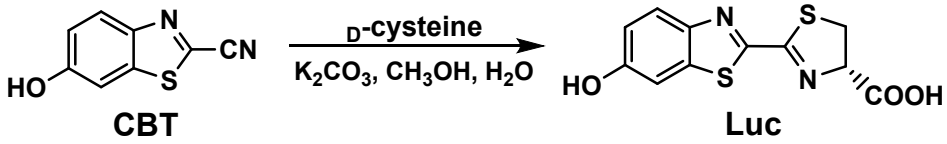


***Scheme S2.*** Synthetic route for **P-Bz-Luc**.

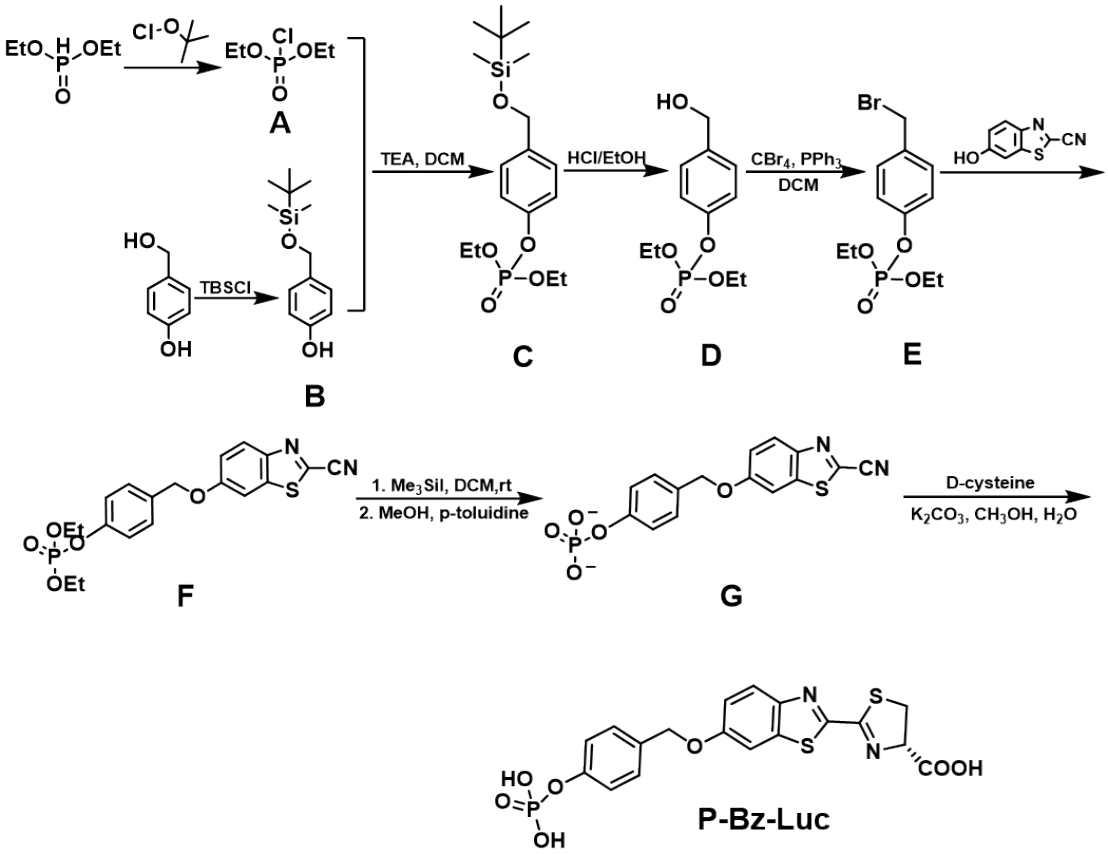

## 2. Supporting Figures and Tables

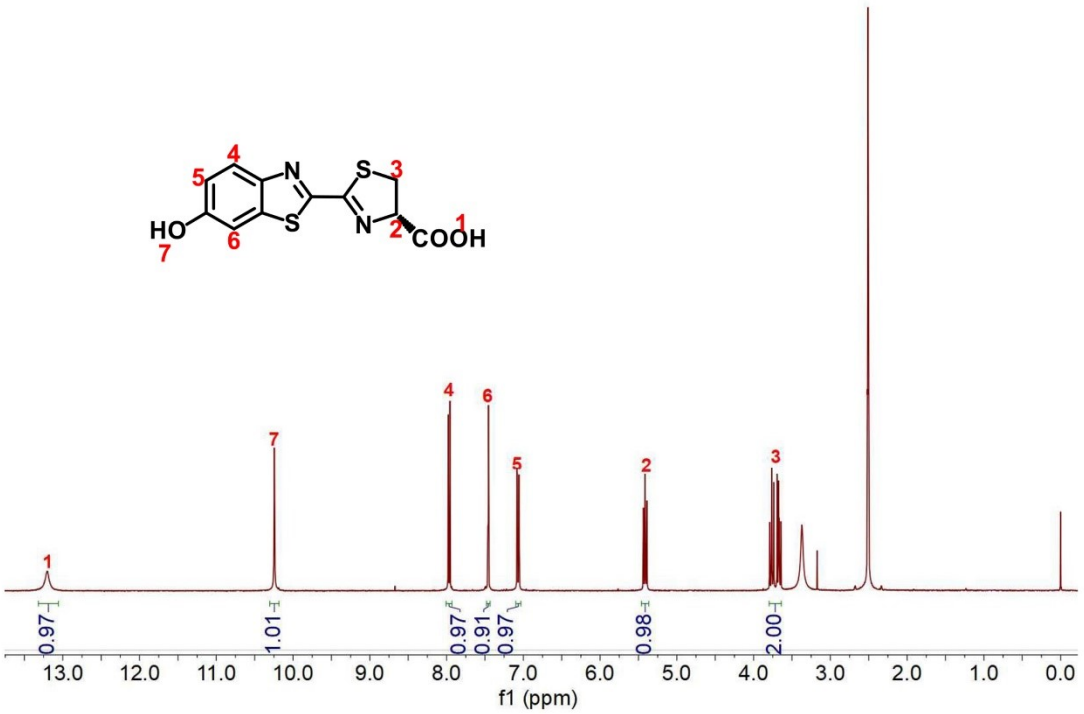


***Figure S1.*** $^{1}$H NMR spectrum of Luc in DMSO-$d_6$.

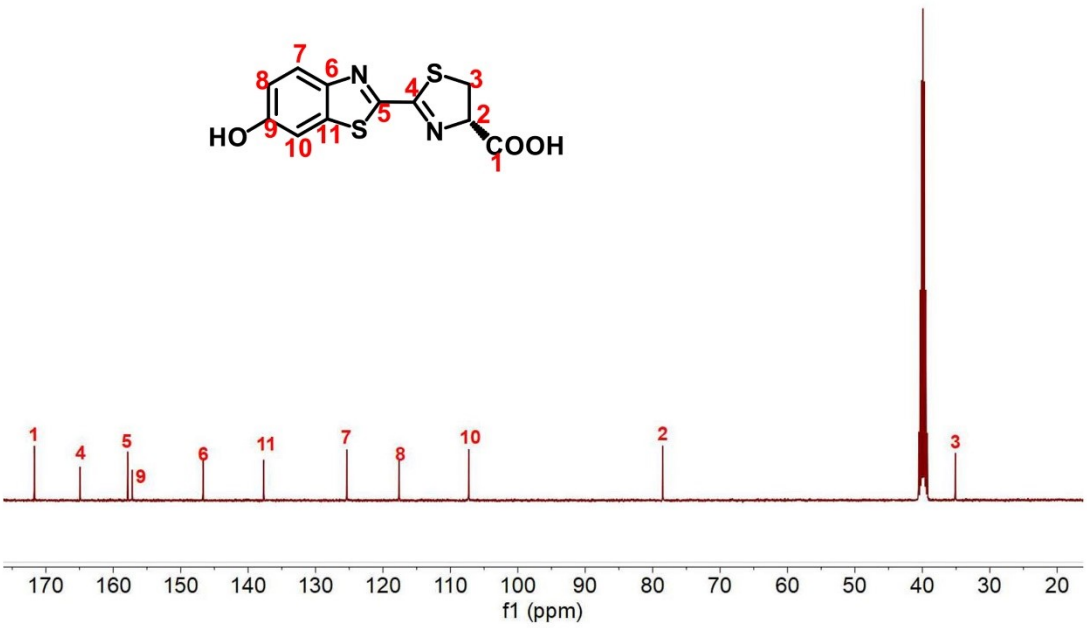


***Figure S2.*** $^{13}$C NMR spectrum of Luc in DMSO-$d_6$.

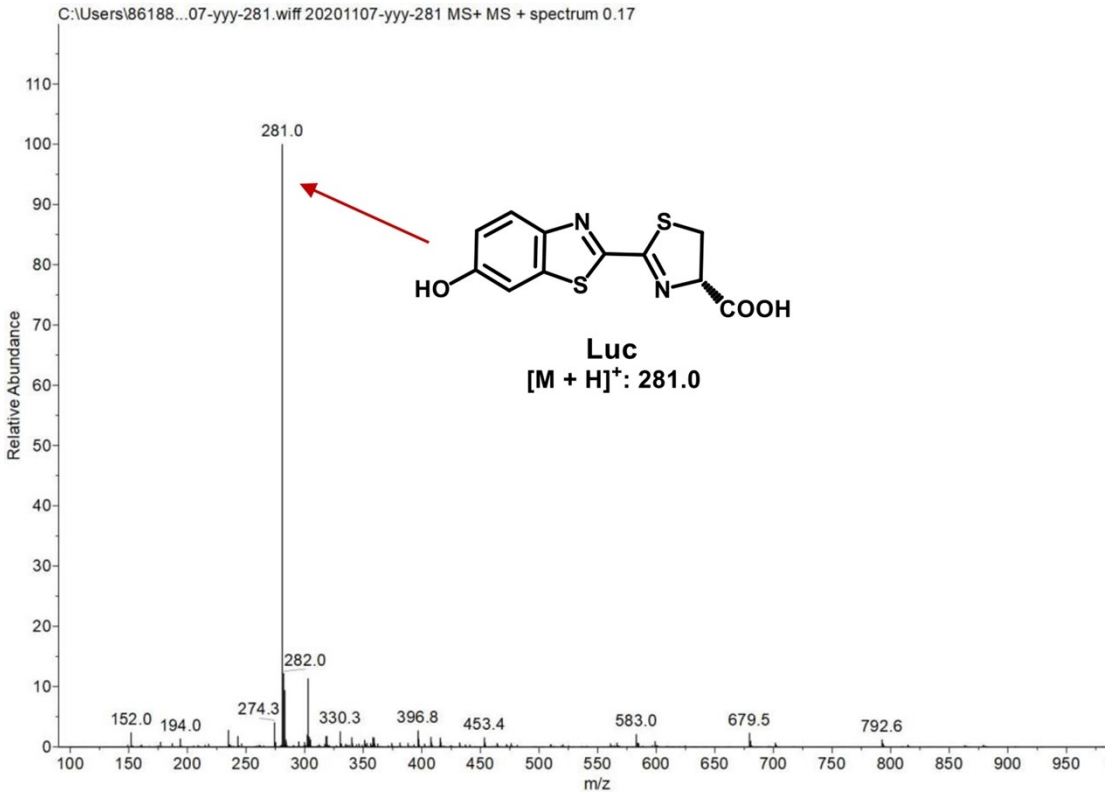


***Figure S3.*** ESI-MS spectrum of Luc.

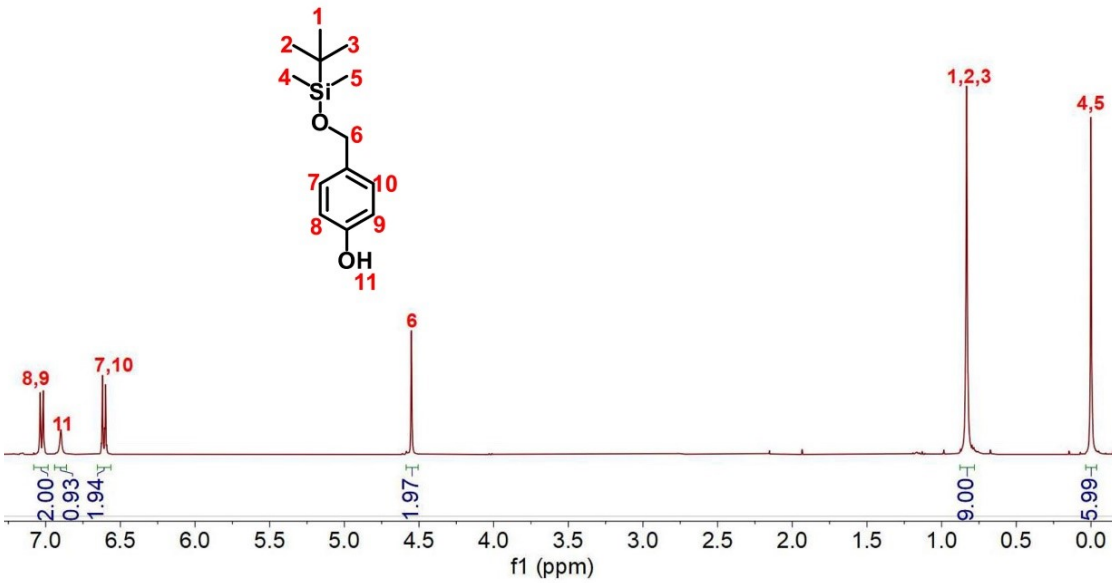


***Figure S4.*** $^{1}H$ NMR spectrum of B in $CDCl_3$.

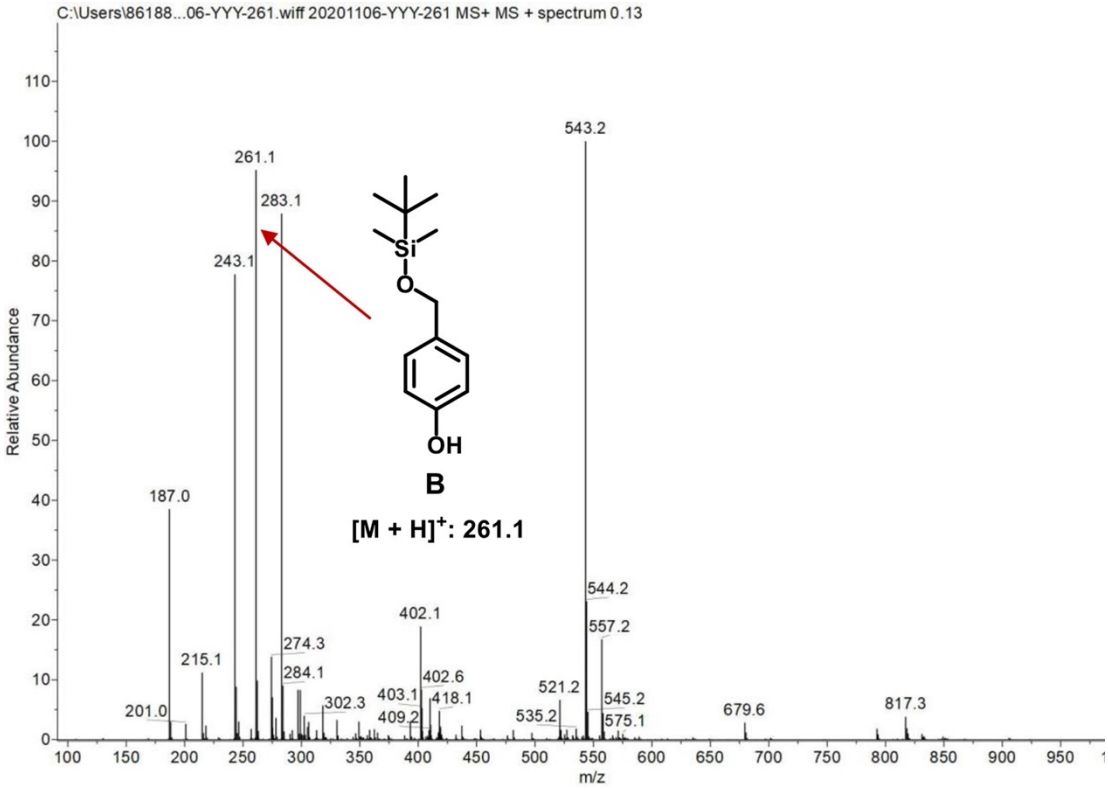


***Figure S5.*** ESI-MS spectrum of B.

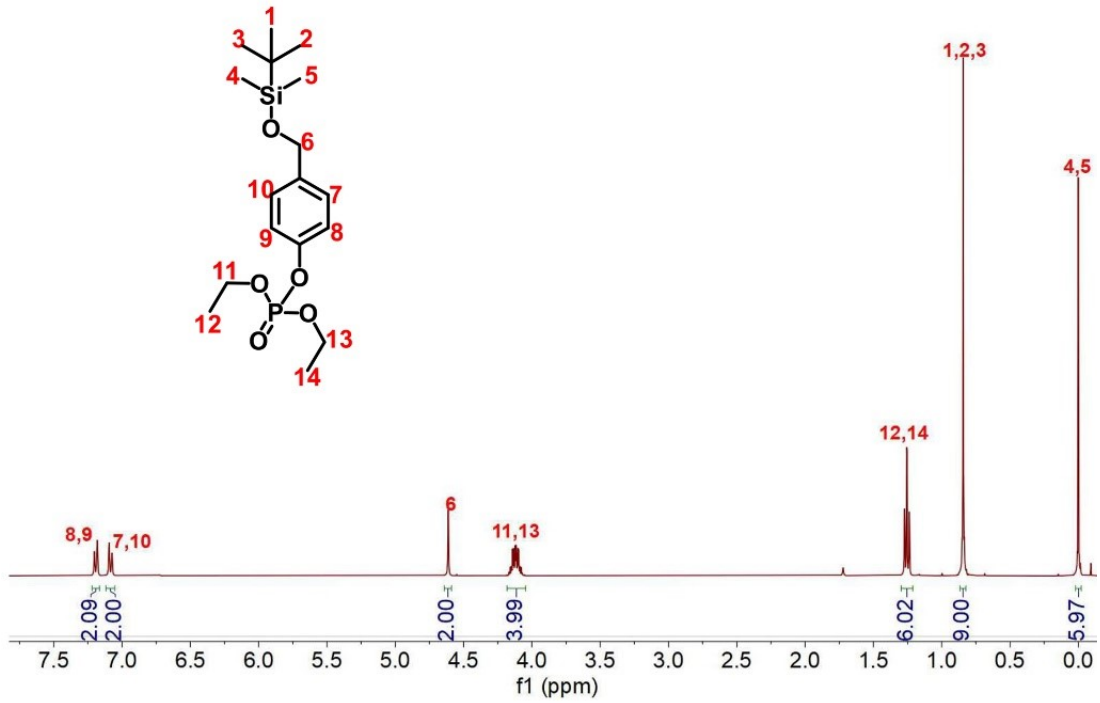


***Figure S6.*** $^{1}H$ NMR spectrum of C in $CDCl_3$.

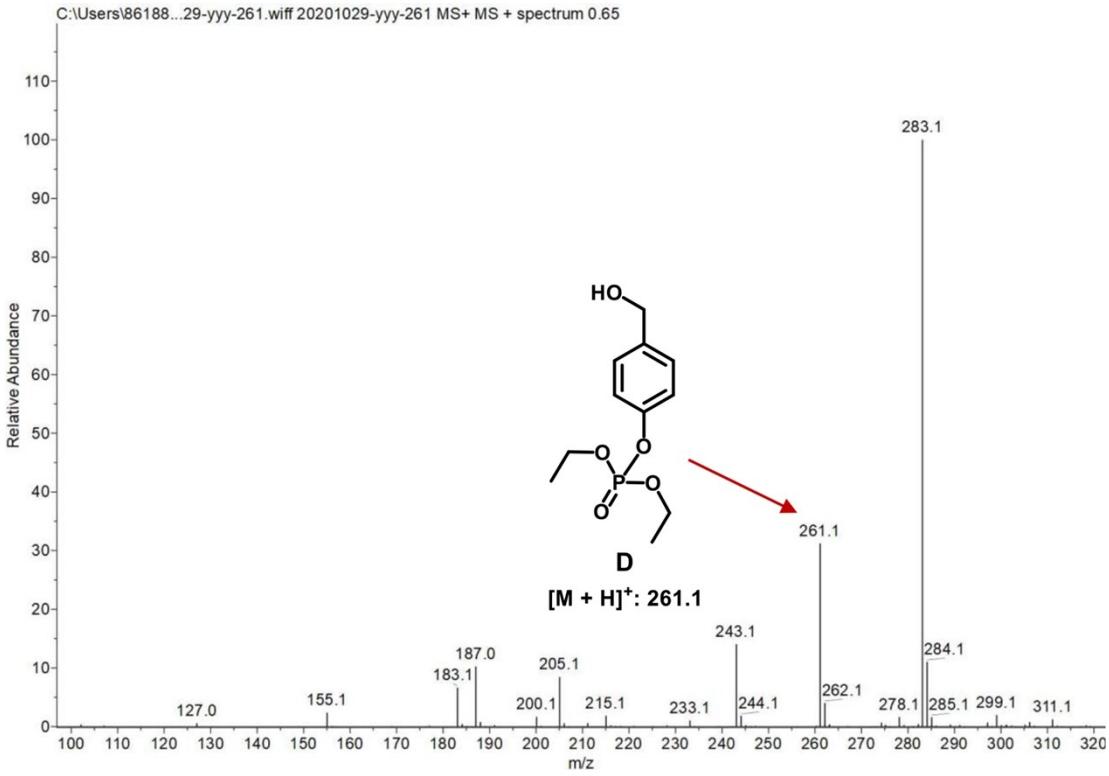


***Figure S7.*** ESI-MS spectrum of D.

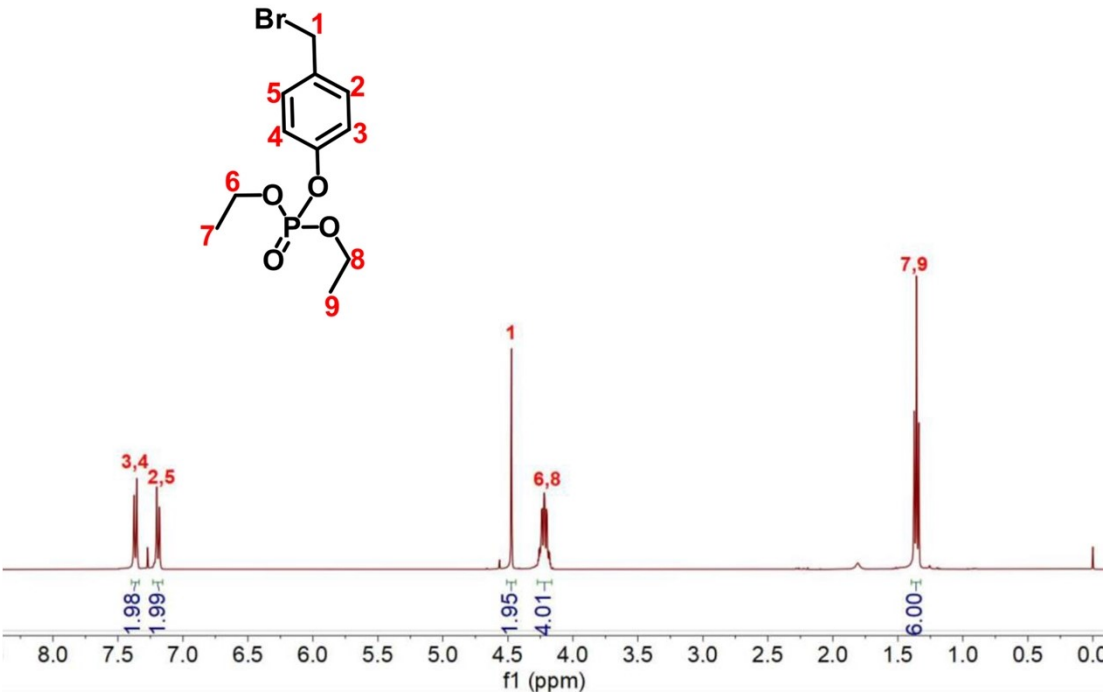


***Figure S8.*** $^{1}$H NMR spectrum of E in $CDCl_3$.

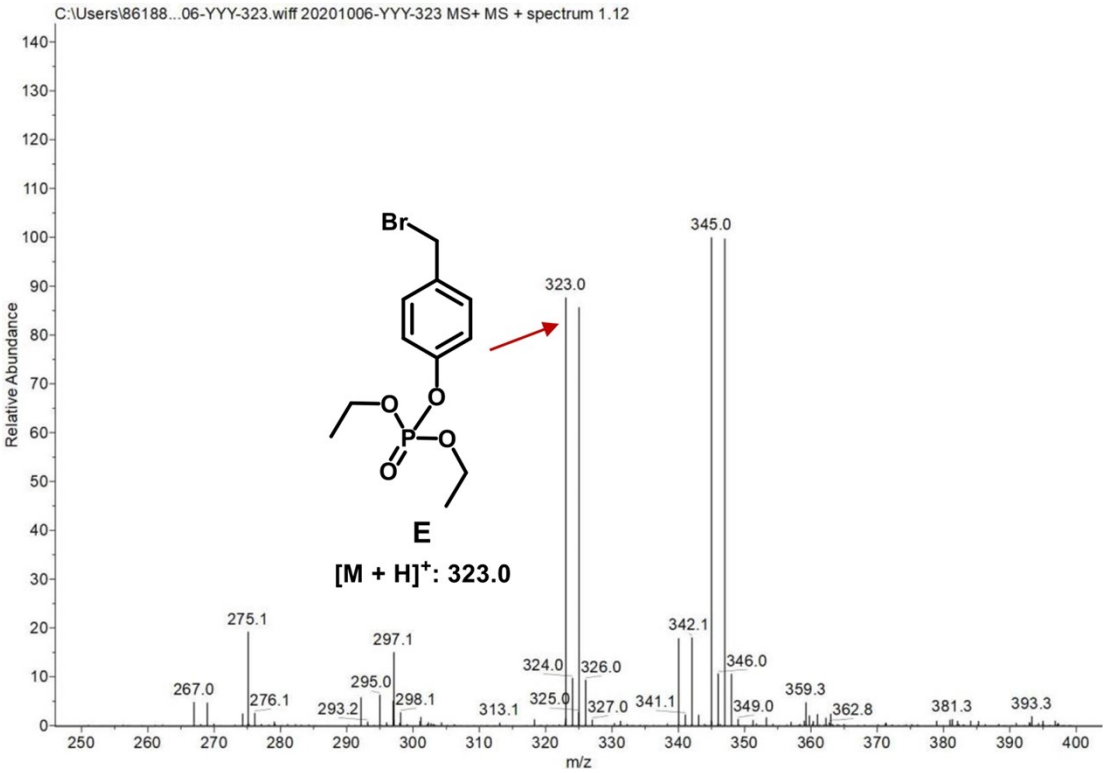


***Figure S9.*** ESI-MS spectrum of E.

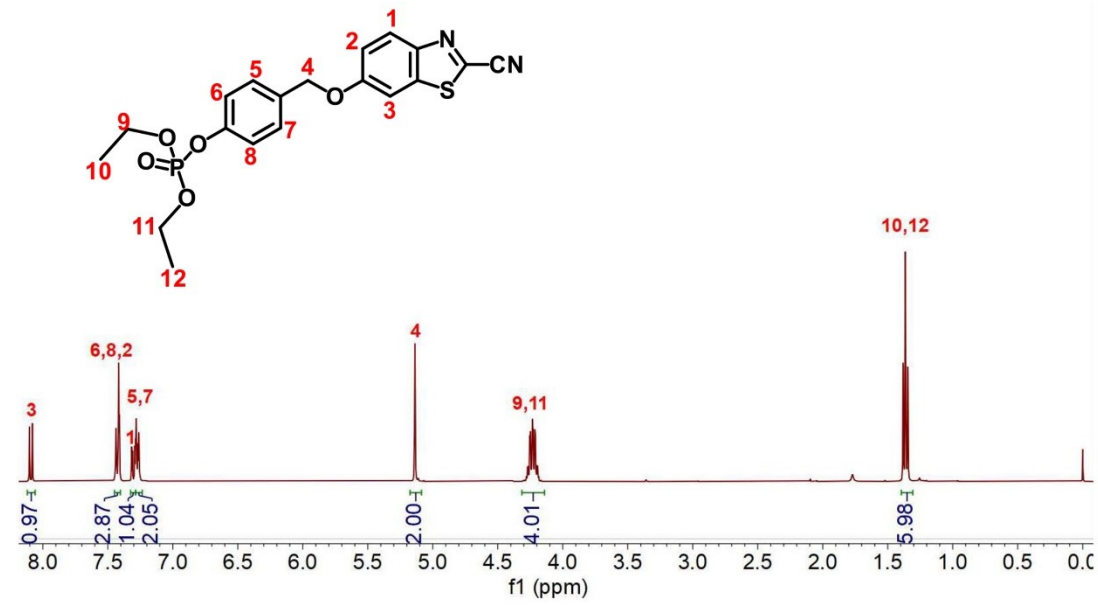


***Figure S10.*** $^{1}$H NMR spectrum of F in $CDCl_3$.

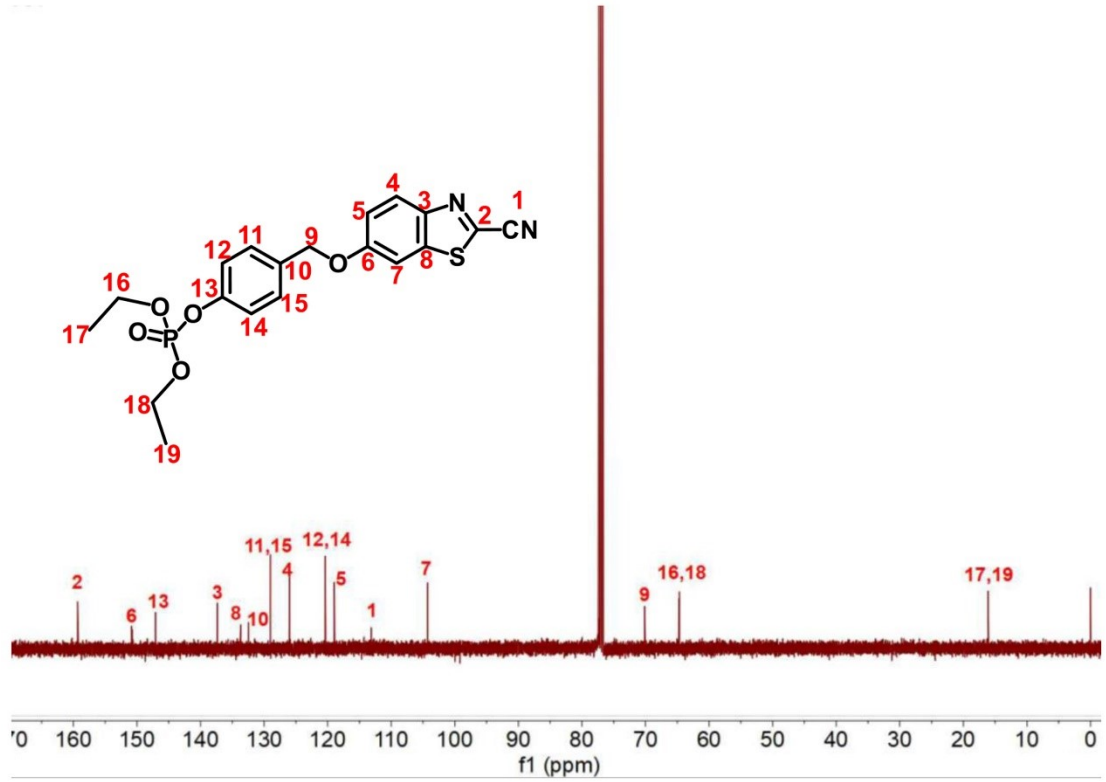


***Figure S11.*** *$^{13}C$* NMR spectrum of F in $CDCl_3$.

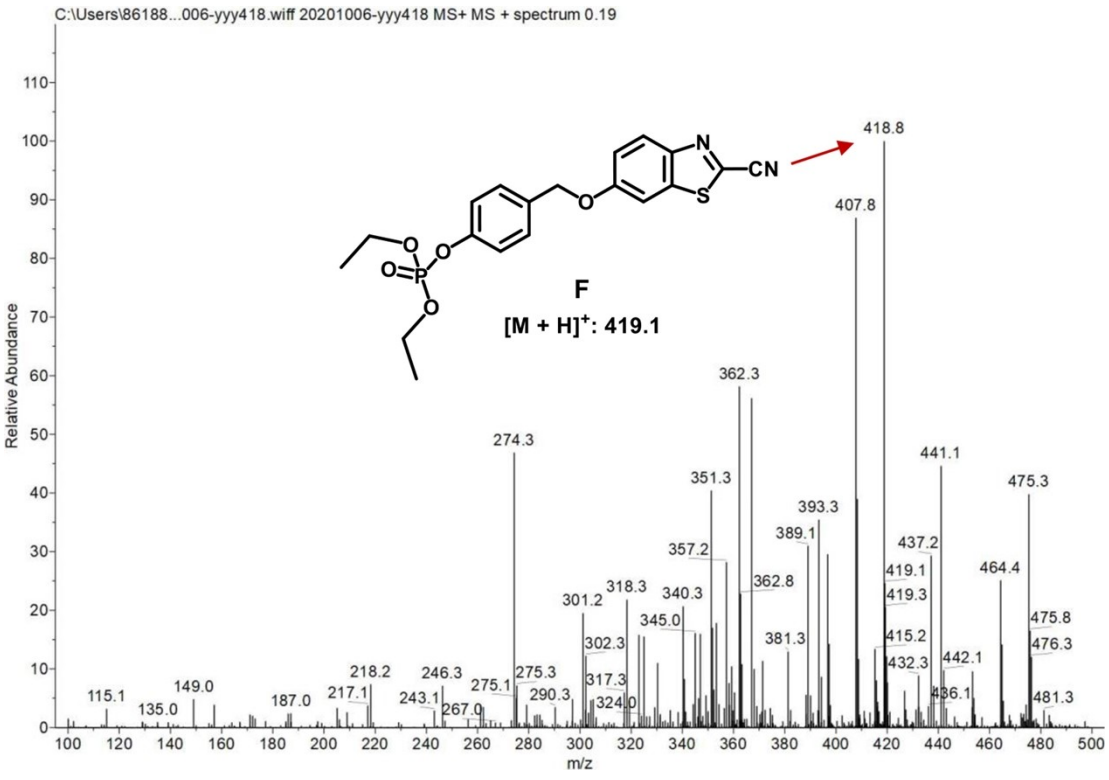


***Figure S12.*** ESI-MS spectrum of F.

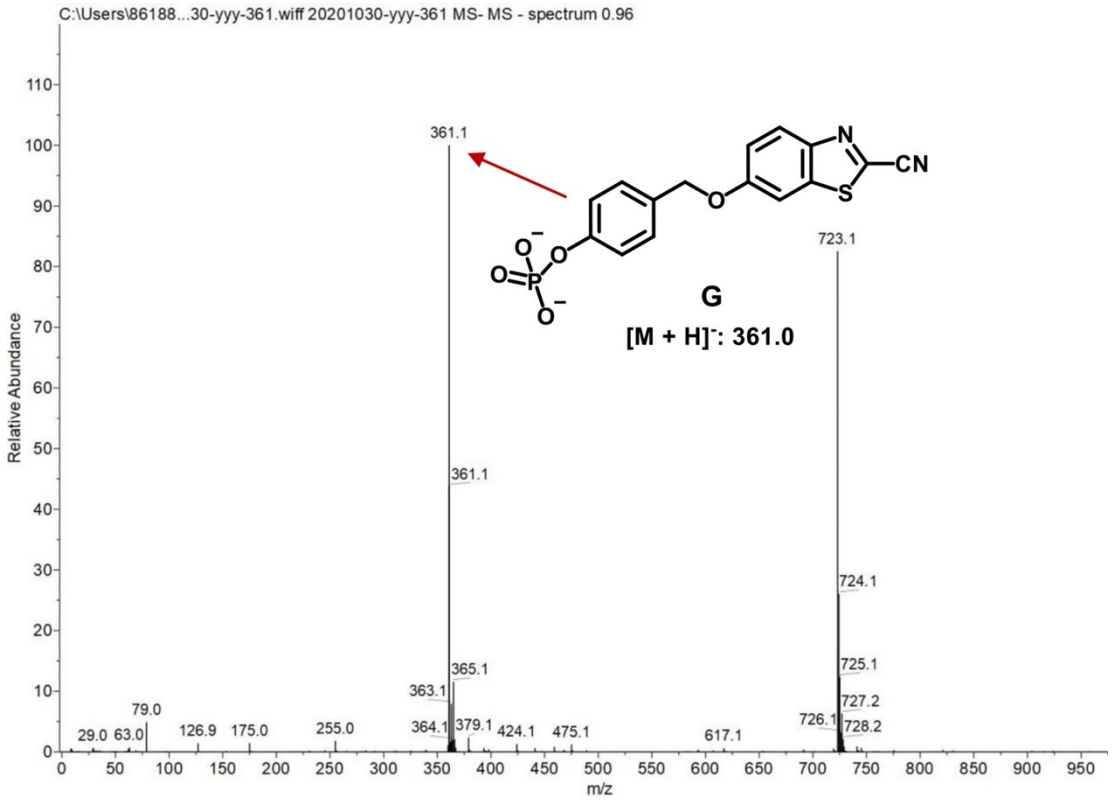


***Figure S13.*** ESI-MS spectrum of G.

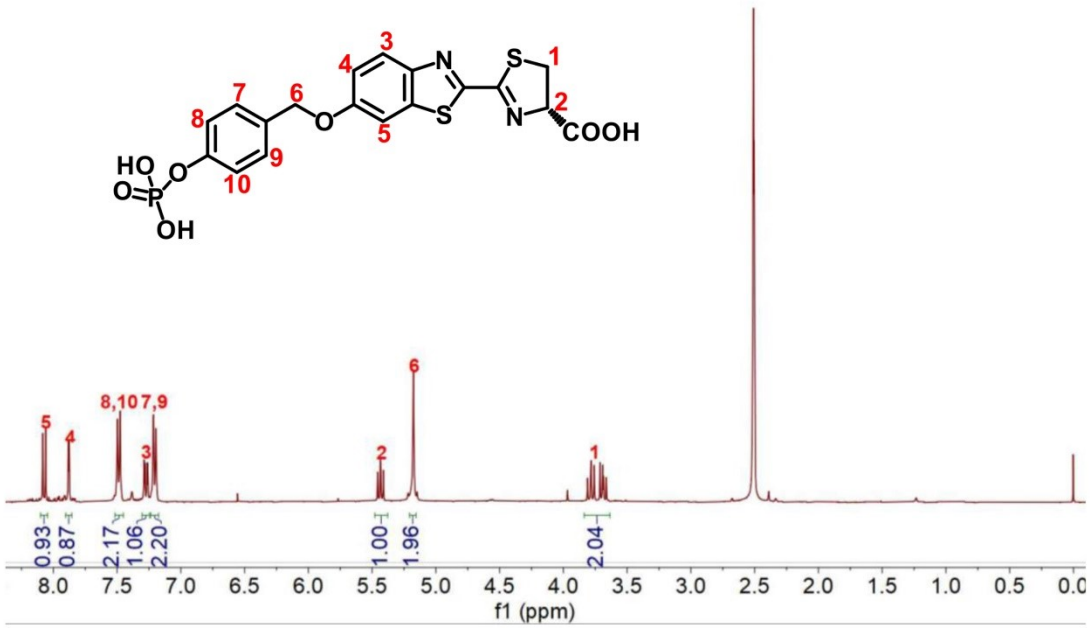


***Figure S14.*** $^{1}$H NMR spectrum of **P-Bz-Luc** in DMSO-$d_6$.

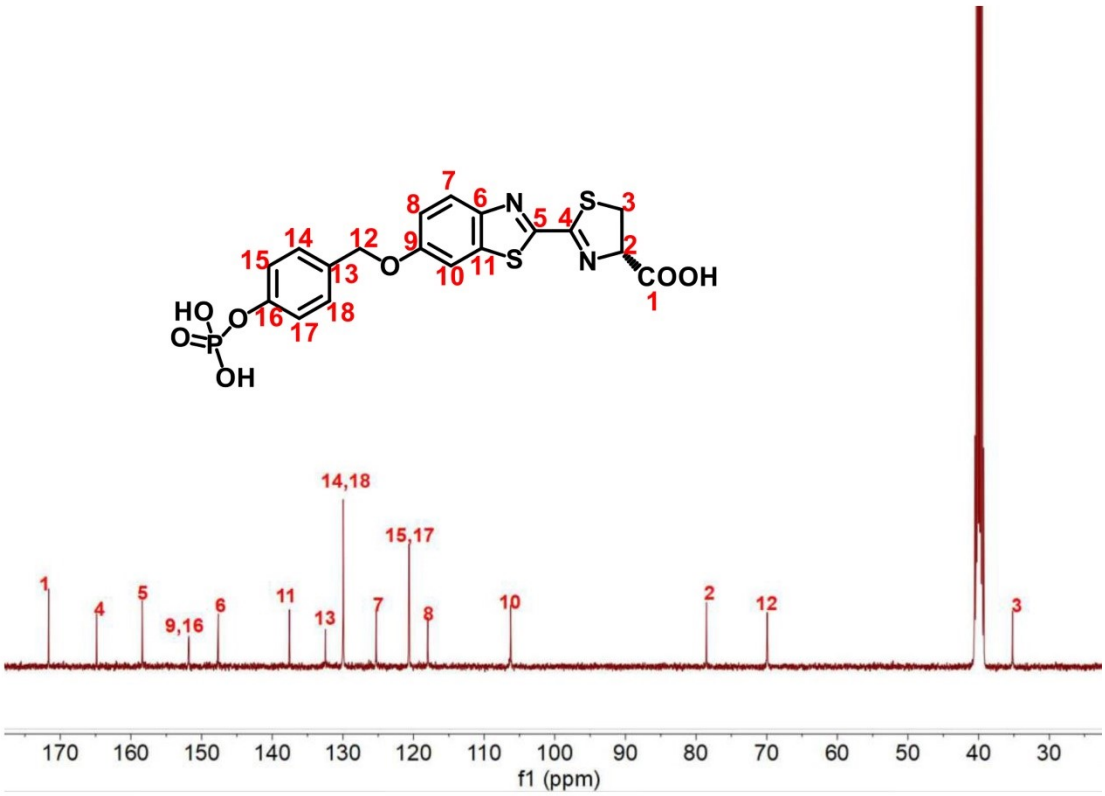


***Figure S15.*** $^{13}$C NMR spectrum of **P-Bz-Luc** in DMSO-$d_6$.

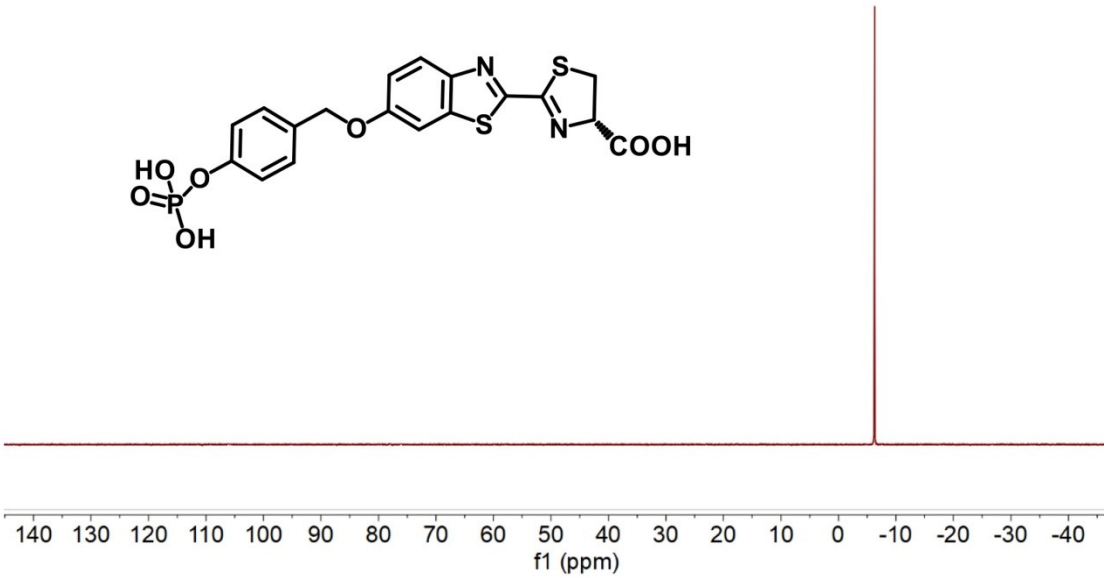


***Figure S16.*** $^{31}$P NMR spectrum of **P-Bz-Luc** in DMSO-$d_6$.

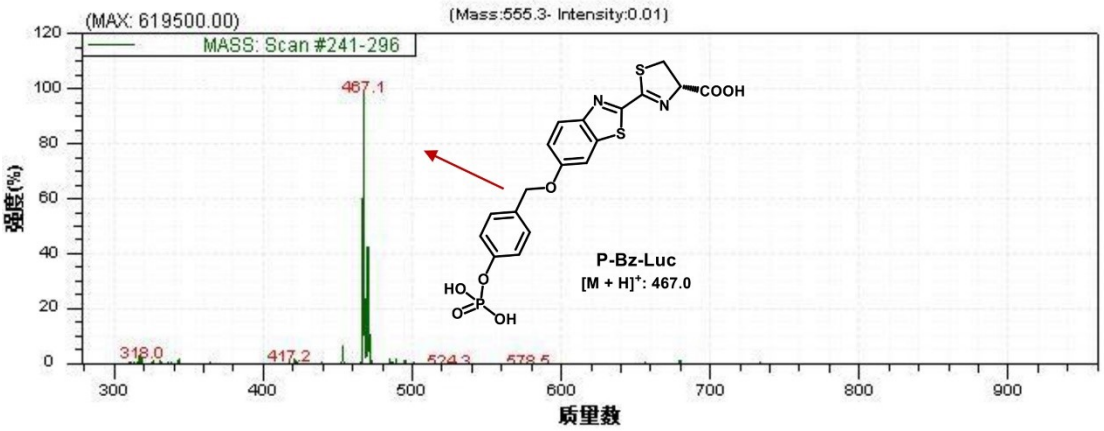


***Figure S17.*** ESI-MS spectrum of **P-Bz-Luc**.

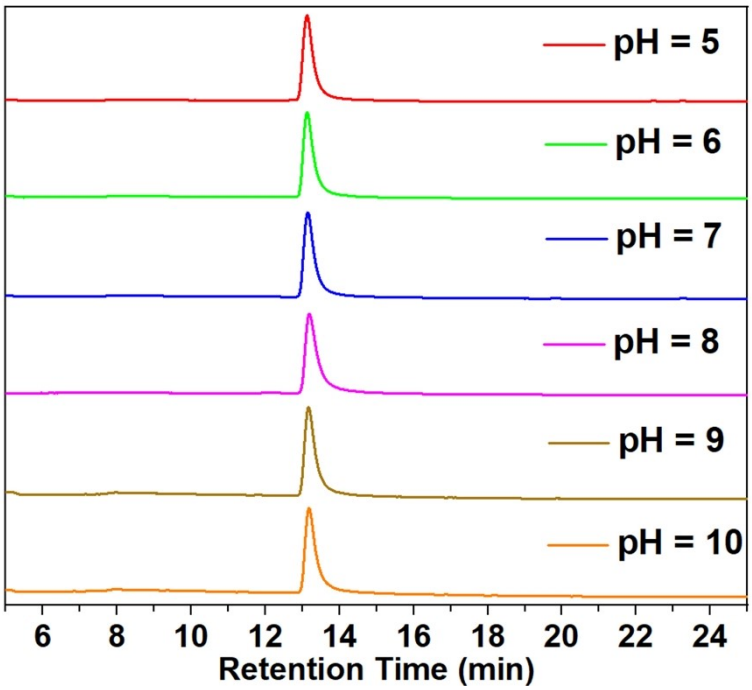


***Figure S18.*** The stability of **P-Bz-Luc** in working buffer at 37 °C and different pH values for 2 h.

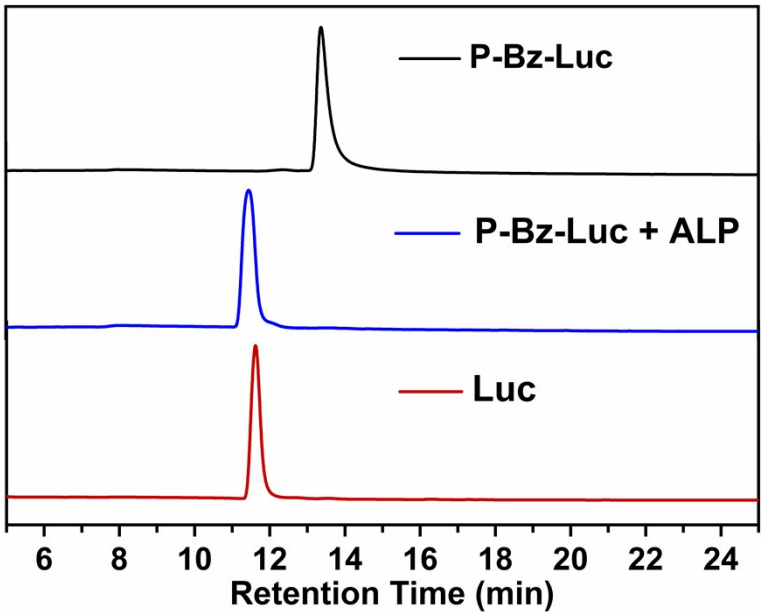


***Figure S19.*** HPLC traces of 25 μM **P-Bz-Luc** (black), 25 μM **P-Bz-Luc** in working buffer (10 mM Tris, pH 8.0) incubated with 100 U/L ALP at 37 °C for 2 h (blue), and 25 μM Luc (red). Wavelength for detection: 320 nm

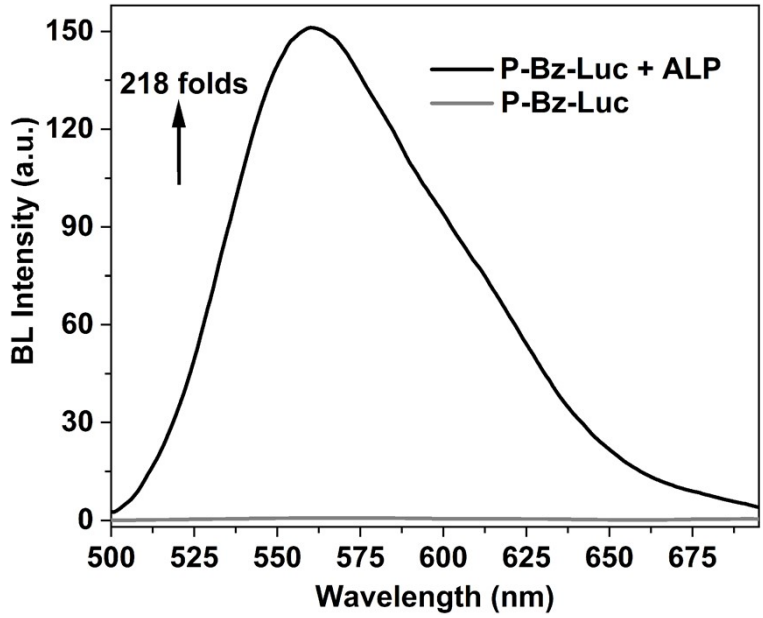


***Figure S20.*** BL spectra of **P-Bz-Luc** (25 μM) before (grey) and after the treatment of ALP (100 U/L) at 37 ℃ for 2 h (black).

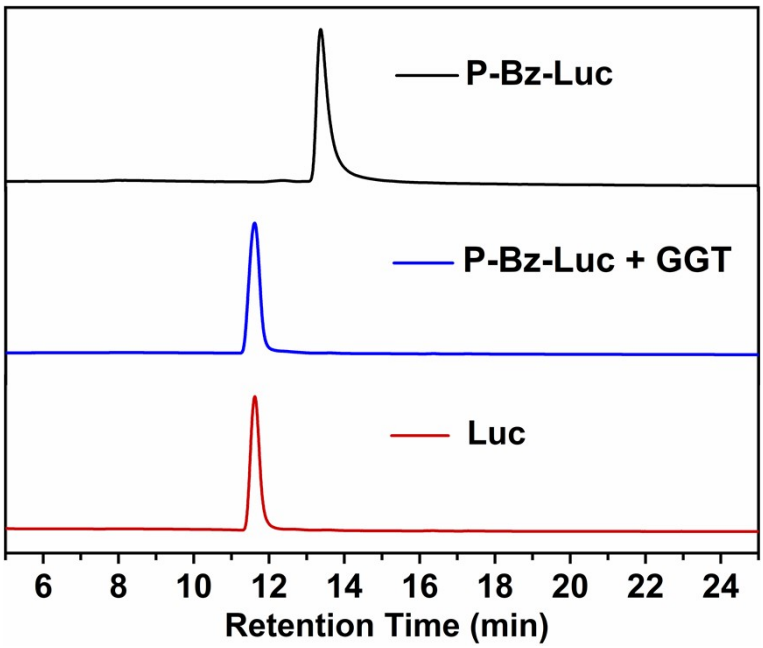


***Figure S21.*** HPLC traces of 25 μM **P-Bz-Luc** (black), 25 μM **P-Bz-Luc** in working buffer (10 mM Tris, pH 8.0) incubated with 200 U/L GGT at 37 °C for 2 h (blue), and 25 μM Luc (red). Wavelength for detection: 320 nm.

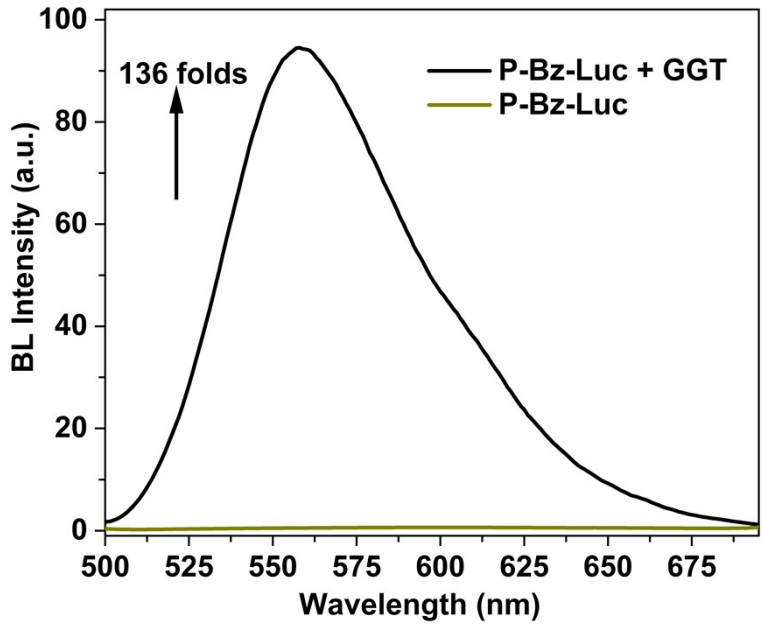


***Figure S22.*** BL spectra of **P-Bz-Luc** (25 μM) before (dark yellow) and after the treatment of GGT (200 U/L) at 37 ℃ for 2 h (black).

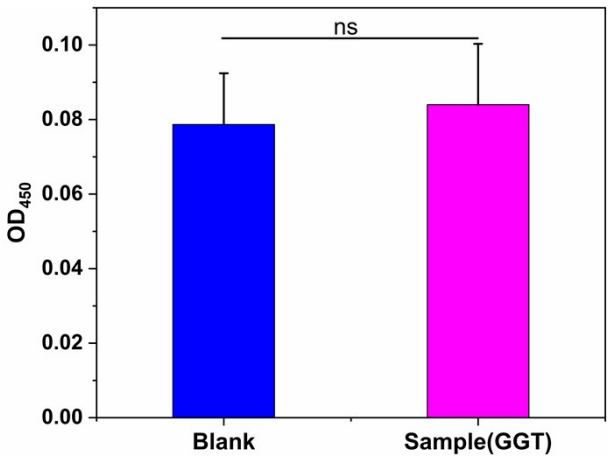


***Figure S23.*** Detection of ALP in the supplied GGT with the horse IgG ELISA kit. The error bar represents the standard deviation of three independent experiments.

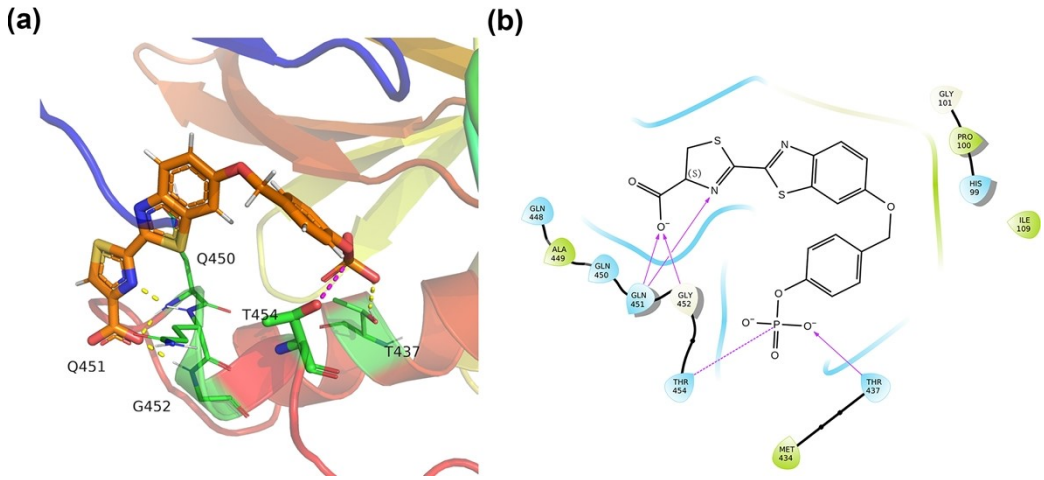


***Figure S24.*** Interactions of **P-Bz-Luc** and GGT6. (a) 3D interaction, hydrogen bonds are highlighted by yellow dash line. Covalent bond is shown as orange dash line. **P-Bz-Luc** is shown as orange stick, GGT6 protein is shown as rainbow cartoon. Pictures were produced by open-source program PyMOL. (b) 2D interaction diagram. Covalent bond is shown as purple dash line, hydrogen bond is shown as violet arrows. Hydrophobic residues are colored by light green and polar residues are colored by light cyan. Pictures were produced by open-source program PyMOL and academic free Maestro.

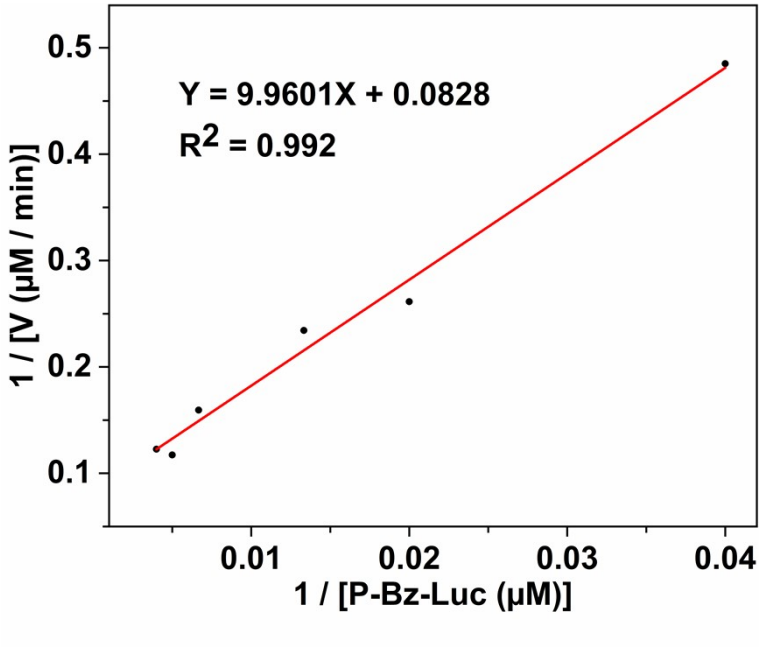


***Figure S25.*** Lineweaver-Burk plots for the ALP enzyme-catalyzed reaction of **P-Bz-Luc**. Conditions: 100 U/L ALP, 25-250 μM of **P-Bz-Luc**.

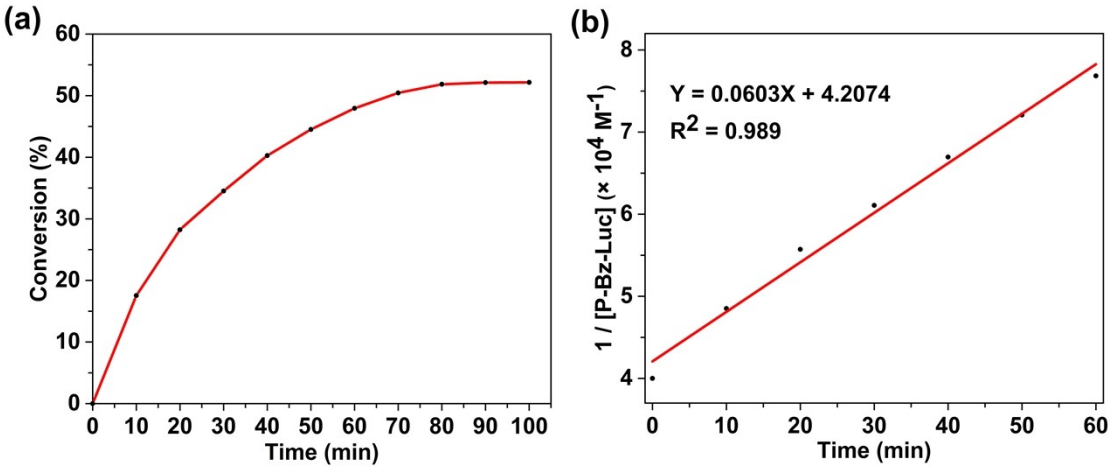


***Figure S26.*** (a) The conversion rate of the reaction between **P-Bz-Luc** and GGT versus the reaction time. (b) Linear regression analysis of the reciprocal remained **P-Bz-Luc** concentration versus the reaction time. Conditions: 100 U/L GGT, 25 μM of

**P-Bz-Luc**.

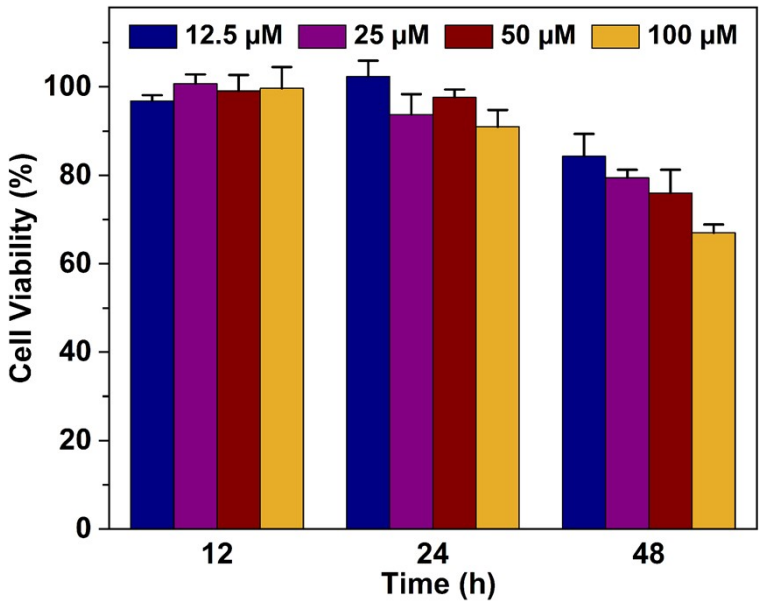


***Figure S27.*** MTT assay of **P-Bz-Luc** on MDA-MB-231 cells (non-luciferase transfected). The error bar represents the standard deviation of three independent experiments.

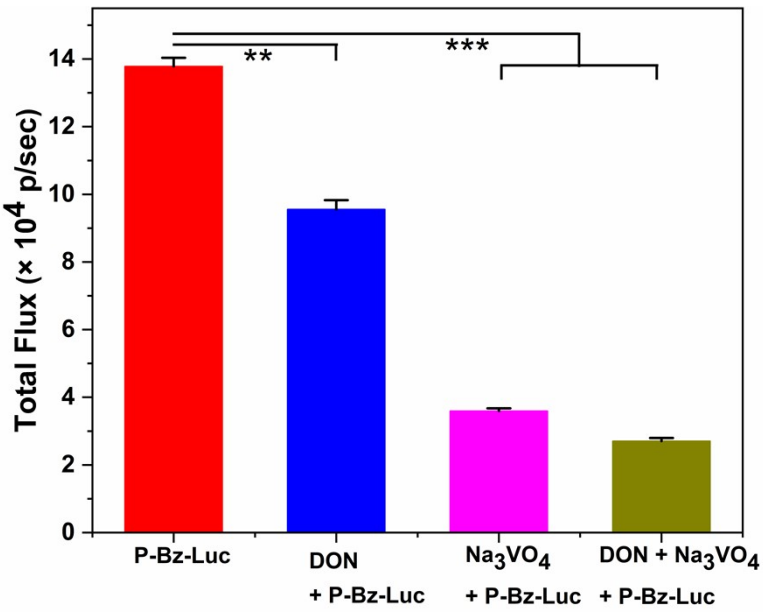


***Figure S28.*** Quantified total photon output of Figure 3a at 10 h; Statistical significance was calculated via Student's t test (** for $P = 0.005$).

***Table S1.*** Summary of detection techniques and limits of detection for **P-Bz-Luc** and recently reported ALP probes.

| Probes | Detection Methods | LOD of ALP |
|---|---|---|
| **P-Bz-Luc** in this work | bioluminescence | 0.172 U/L |
| LET-3 | near infrared fluorescence | 0.200 U/L [1] |
| FAS-P | aggregation induced emission | 0.600 U/L [2] |
| MTR-P | near infrared fluorescence | 0.0420 U/L [3] |
| CyP | fluorescence | 0.730 U/L [4] |
| P-TPE-TG | ratiometric fluorescence | 0.0340 U/L [5] |
| DQM-ALP | aggregation induced emission | 0.150 U/L [6] |
| APW | ratiometric fluorescence | 0.460 U/L [7] |
| Cy-OP | near infrared fluorescence | 0.160 U/L [8] |

***Table S2.*** Summary of detection techniques and limits of detection for **P-Bz-Luc** and recently reported GGT probes.

| Probes | Detection Methods | LOD of GGT |
|---|---|---|
| **P-Bz-Luc** in this work | bioluminescence | 0.634 U/L |
| Cy-GSH | ratiometric near-infrared fluorescence | 0.0300 U/L [9] |
| ABTT-Glu | aggregation induced emission | 2.90 U/L [10] |
| TMN-Glu | near infrared fluorescence | 0.0240 U/L [11] |
| Mito-Bcy-GGT | near infrared fluorescence | 0.400 U/L [12] |
| NIR-SN-GGT | near infrared fluorescence | 0.0240 U/L [13] |
| mNVPy_Glu | fluorescence | 1.47 U/L [14] |
| DPP-GGT | ratiometric fluorescence | 0.154 U/L [15] |

## 3. References

(1)Gao, X.; Ma, G.; Jiang, C.; Zeng, L.; Jiang, S.; Huang, P.; Lin, J., In Vivo Near-Infrared Fluorescence and Photoacoustic Dual-Modal Imaging of Endogenous Alkaline Phosphatase. *Anal. Chem.* **2019,** *91* (11), 7112-7117.

(2)Li, Y.; Xie, R.; Pang, X.; Zhou, Z.; Xu, H.; Gu, B.; Wu, C.; Li, H.; Zhang, Y., Aggregation-induced emission fluorescent probe for monitoring endogenous alkaline phosphatase in living cells. *Talanta* **2019,** *205*, 120143.

(3)Xu, L.; He, X.; Huang, Y.; Ma, P.; Jiang, Y.; Liu, X.; Tao, S.; Sun, Y.; Song, D.; Wang, X., A novel near-infrared fluorescent probe for detecting intracellular alkaline phosphatase and imaging of living cells. *J. Mater. Chem. B.* **2019,** *7* (8), 1284-1291.

(4)Sun, J.; Liu, M.; Wang, P.; Gao, Z.; Mu, J.; Chen, Q., Novel High-Selectivity Fluorescent Probe for Detecting Alkaline Phosphatase Activity in Marine Environment. *J. Nanosci. Nanotechnol.* **2020,** *20* (6), 3348-3355.

(5)Lee, J.; Kim, S.; Kim, T. H.; Lee, S. H., A ratiometric fluorescence sensor based on enzymatically activatable micellization of TPE derivatives for quantitative detection of alkaline phosphatase activity in serum. *RSC Advances* **2020,** *10* (45), 26888-26894.

(6)Li, H.; Yao, Q.; Xu, F.; Li, Y.; Kim, D.; Chung, J.; Baek, G.; Wu, X.; Hillman, P. F.; Lee, E. Y.; Ge, H.; Fan, J.; Wang, J.; Nam, S. J.; Peng, X.; Yoon, J., An Activatable AIEgen Probe for High-Fidelity Monitoring of Overexpressed Tumor Enzyme Activity and Its Application to Surgical Tumor Excision. *Angew. Chem. Int. Ed.* **2020,** *59* (25), 10186-10195.

(7)Zhang, X.; Chen, X.; Zhang, Y.; Gao, G.; Huang, X.; Hou, S.; Ma, X., A high-sensitivity fluorescent probe with a self-immolative spacer for real-time ratiometric detection and imaging of alkaline phosphatase activity. *New Journal of Chemistry* **2019,** *43* (30), 11887-11892.

(8)Zhang, Q.; Li, S.; Fu, C.; Xiao, Y.; Zhang, P.; Ding, C., Near-infrared mito-specific fluorescent probe for ratiometric detection and imaging of alkaline phosphatase activity with high sensitivity. *J. Mater. Chem. B.* **2019,** *7* (3), 443-450.

(9)Ou-Yang, J.; Li, Y.; Jiang, W. L.; He, S. Y.; Liu, H. W.; Li, C. Y., Fluorescence-Guided Cancer Diagnosis and Surgery by a Zero Cross-Talk Ratiometric Near-Infrared gamma-

Glutamyltranspeptidase Fluorescent Probe. *Anal. Chem.* **2019,** *91* (1), 1056-1063.

(10)Liu, Y.; Feng, B.; Cao, X.; Tang, G.; Liu, H.; Chen, F.; Liu, M.; Chen, Q.; Yuan, K.; Gu, Y.; Feng, X.; Zeng, W., A novel "AIE + ESIPT" near-infrared nanoprobe for the imaging of gamma-glutamyl transpeptidase in living cells and the application in precision medicine. *Analyst* **2019,** *144* (17), 5136-5142.

(11)Liu, F.; Wang, Z.; Zhu, T.; Wang, W.; Nie, B.; Li, J.; Zhang, Y.; Luo, J.; Kong, L., Real-time monitoring of gamma-Glutamyltranspeptidase in living cells and in vivo by near-infrared fluorescent probe with large Stokes shift. *Talanta* **2019,** *191*, 126-132.

(12)Liu, H.; Liu, F.; Wang, F.; Yu, R. Q.; Jiang, J. H., A novel mitochondrial-targeting near-infrared fluorescent probe for imaging gamma-glutamyl transpeptidase activity in living cells. *Analyst* **2018,** *143* (22), 5530-5535.

(13)Li, H.; Yao, Q.; Xu, F.; Xu, N.; Sun, W.; Long, S.; Du, J.; Fan, J.; Wang, J.; Peng, X., Lighting-Up Tumor for Assisting Resection via Spraying NIR Fluorescent Probe of gamma-Glutamyltranspeptidas. *Front. Chem.* **2018,** *6*, 485.

(14)Reo, Y. J.; Dai, M.; Yang, Y. J.; Ahn, K. H., Cell-Membrane-Localizing, Two-Photon Probe for Ratiometric Imaging of gamma-Glutamyl Transpeptidase in Cancerous Cells and Tissues. *Anal. Chem.* **2020,** *92* (18), 12678-12685.

(15)Yang, Z.; Xu, W.; Wang, J.; Liu, L.; Chu, Y.; Wang, Y.; Hu, Y.; Yi, T.; Hua, J., Diketopyrrolopyrrole-based multifunctional ratiometric fluorescent probe and γ-glutamyltranspeptidase-triggered activatable photosensitizer for tumor therapy. *J. Mater. Chem. B.* **2020,** *8* (24), 8183-8190.